Direct antiviral activity of interferon stimulated genes is responsible for resistance to paramyxoviruses in ISG15-deficient cells

David Holthaus[1]*‡, Andri Vasou[1]*, Connor G. G. Bamford[2]‡, Jelena Andrejeva[1], Christina Paulus[1], Richard E. Randall[1], John McLauchlan[2], David J. Hughes[1]†

[1]Biomedical Sciences Research Complex, School of Biology, University of St Andrews, St Andrews, United Kingdom. [2]MRC-University of Glasgow Centre for Virus Research, Glasgow, United Kingdom.

*These authors contributed equally.

‡ Present addresses: (DH) Unit 16 Mycotic and Parasitic Agents and Mycobacteria, Robert Koch-Institute, Berlin, Germany. (CGGB) Wellcome-Wolfson Institute for Experimental Medicine, Queen's University, Belfast UK.

†Corresponding author: djh25@st-andrews.ac.uk; Tel: +44 1334 467197.

Abstract

Interferons (IFNs), produced during viral infections, induce the expression of hundreds of IFN-stimulated genes (ISGs). Some ISGs have specific antiviral activity while others regulate the cellular response. In addition to functioning as an antiviral effector, IFN-stimulated gene 15 (ISG15) is a negative regulator of IFN signalling and inherited ISG15-deficiency leads to autoinflammatory interferonopathies where individuals exhibit elevated ISG expression in the absence of infection. We have recapitulated these effects in cultured human A549-ISG15$^{-/-}$ cells and (using A549-UBA7$^{-/-}$ cells) confirmed that posttranslational modification by ISG15 (ISGylation) is not required for regulation of the type-I IFN response. ISG15-deficient cells pre-treated with IFN-α were resistant to paramyxovirus infection. We also showed that IFN-α treatment of ISG15-deficient cells led to significant inhibition of global protein synthesis leading us to ask whether resistance was due to the direct antiviral activity of ISGs or whether cells were non-permissive due to translation defects. We took advantage of the knowledge that IFN-induced protein with tetratricopeptide repeats 1 (IFIT1) is the principal antiviral ISG for parainfluenza virus 5 (PIV5). Knockdown of IFIT1 restored PIV5 infection in IFN-α-pre-treated ISG15-deficient cells, confirming that resistance was due to the direct antiviral activity of the IFN response. However, resistance could be induced if cells were pre-treated with IFN-α for longer times, presumably due to inhibition of protein synthesis. These data show that the cause of virus resistance is two-fold; ISG15-deficiency leads to the ‘early' over-expression of specific antiviral ISGs, but the later response is dominated by an unanticipated, ISG15-dependent, loss of translational control.

38 **Introduction**

39 The innate immune response against pathogens is underpinned by the evolutionary conserved
40 interferon (IFN) system. All cells express pathogen recognition receptors (PRRs) that sense the
41 products of infection and establish a signalling cascade leading to the production of cytokines,
42 including type I IFN (IFN-α/β) (1, 2). IFN is secreted from cells and binds to cell surface receptors
43 expressed on both infected and non-infected cells, initiating a JAK/STAT signalling cascade,
44 culminating in the expression of hundreds of interferon stimulated genes (ISGs) (3). The biological
45 effects of ISGs are extensive and their principle role is to generate an unfavourable environment for
46 the replication of viruses. Many ISGs have broad antiviral activity, such as double-stranded RNA
47 dependent protein kinase (PKR) that, upon recognition of viral dsRNA, dampens general protein
48 synthesis and prevents the translation of viral mRNAs (4). Other antiviral ISGs, such as IFN-induced
49 protein with tetratricopeptide repeats (IFIT) proteins, inhibit specific viruses, but for many, they are
50 inconsequential (5). Additionally, multiple ISGs are generally required to limit infection because the
51 majority of ISGs result in low to moderate levels of inhibition (6); however, ISGs with specific
52 antiviral properties for a given virus are usually not known. Nevertheless, the nature of the innate
53 immune response necessitates the production of the complete spectrum of ISGs, albeit with a high
54 degree of redundancy, as during a natural infection, the identity of the infecting virus is not known.
55 This response is inevitably tightly regulated, as a dysregulated response leads to a suite of
56 autoinflammatory diseases (7).

57 The ubiquitin-like protein (Ubl) ISG15 is strongly induced by IFN and is critical for regulating how cells
58 respond to infection. As a posttranslational modification (PTM), it can covalently modify proteins in a
59 process known as ISGylation, and in many cases, modification of viral proteins forms part of the
60 antiviral response (8). Covalently bound ISG15 can also be removed from proteins by the ubiquitin
61 specific protease USP18 (9). Importantly, loss-of-function mutations in ISG15 have been identified in
62 human patients with subsets of autoinflammatory interferonopathies and typically these individuals

63 demonstrate elevated ISG expression in the absence of infection (10). Mechanistically, it was shown
64 that ISG15 functions as a negative regulator of type I IFN signalling by stabilising USP18, a known
65 inhibitor of JAK/STAT signalling (11-13). Intriguingly, despite the known functions of ISG15 and
66 USP18 in the ISGylation process, the regulation of type I IFN signalling was entirely independent of
67 ISGylation (10). Interestingly, mouse Isg15 is not required to stabilise Usp18 and appears not to be
68 needed to regulate IFN signalling, suggesting a species-specific, gain-of-function for human ISG15
69 (although other species have not yet been tested) (14).

70 Previous work has shown that cells from ISG15-deficient patients expressed higher levels of ISGs
71 compared to normal controls when treated with recombinant IFN-α and these cells were resistant to
72 several viruses (14); however, it was not clear at what stage of infection viruses were blocked nor
73 how. Furthermore, cells were treated with IFN-α followed by washing (to remove IFN) and rested for
74 36 hours prior to infection. Since ISG15 is involved in regulating the cell cycle (15) and protein
75 synthesis (shown in this report), an over-amplified IFN response (due to lack of ISG15 and reduced
76 levels of USP18) may have led to virus resistance simply because cells were no longer permissive to
77 infection. This has implications for our understanding as to why ISG15-deficient patients are not
78 more susceptible to viral infections; these observations have led to the suggestion that, unlike in
79 mice, human ISG15 is not an antiviral effector (14, 16).

80 In this study, we recapitulated the phenotype observed in ISG15-deficient patient cells upon
81 treatment with recombinant IFN-α2b in a cell culture model and dissected the mechanisms that
82 result in virus resistance during an antiviral state. We showed that resistance was due to the direct
83 antiviral activity of the type I IFN response and discuss the implications of ISG15-loss-of-function
84 during the innate immune response. Based on our findings, we conclude that observations from
85 ISG15-deficient patients alone cannot be used to infer that ISG15 does not possess antiviral effector
86 functions, as has been proposed (14, 16).

87

88 **Materials and methods**

89 **Cells**

90 Vero cells (African green monkey kidney epithelial cells) and A549 cells (human adenocarcinoma
91 alveolar basal epithelial cells), and derivatives, were maintained in Dulbecco's modified Eagles's
92 medium (DMEM; Sigma) supplemented with 10% (v/v) heat-inactivated foetal bovine serum (FBS,
93 Biowest) and incubated in 5% (v/v) CO_2 at 37°C in a humidified incubator. A549-shIFIT1 have been
94 described elsewhere (17) and were maintained in blasticidin (10 µg/ml). A549-ISG15$^{-/-}$ cells were
95 generated by CRISPR/Cas9n system that utilises the D10A dual 'nickase' mutant of Cas9 (Cas9n) that
96 ostensibly limits off-target effects. Briefly, to disrupt exon 2 of the ISG15 gene, single guide RNA
97 (sgRNA) sequences were cloned using the pPX460 and transfected into A549 cells as previously
98 described (18). Transfectants were enriched after 48 h by treating cells with puromycin (1 µg/ml) for
99 2 d and then diluted to single cells in 96-well plates. Correctly edited cell clones were verified by
100 immunoblot analysis. A549-ISG15$^{-/-}$-shIFIT1 cells were generated as previously described using A549-
101 ISG15$^{-/-}$ (B8) and maintained in media with blasticidin (10 µg/ml) (17). To generate A549-UBA7$^{-/-}$
102 cells, A549 cells were first made to stably express *Streptococcus pyogenes* Cas9 following blasticidin
103 selection of cells transduced with lentiCas9-Blast (gift from Feng Zhang, Addgene plasmid # 52962
104 (19)). The sgRNA sequence that targeted exon 3 of UBA7 was chosen computationally
105 (https://www.deskgen.com) and complementary oligonucleotides (sense:
106 caccGCACACGGGTGACATCACTG; antisense: aaacCAGTGATGTCACCCGTGTGC) were hybridised and
107 ligated into the *Bsm* BI site of pLentiGuide-Puro (gift from Feng Zhang, Addgene # 52963 (20)). Cas9-
108 expressing A549s were transduced with UBA7 sgRNA-expressing lentiGuide-Puro and selected with
109 puromycin. Puromycin-resistant cells were single-cell cloned by FACS and successful knockout cells
110 were validated by immunoblot analysis. A549-Npro cells have been described previously (21).

111 **Virus infections and treatments.**

112 Viruses used were human parainfluenza virus 2 (HPIV2) strain Colindale (HPIV2-Co), HPIV3 strain
113 Washington/47885/57 (HPIV3-Wash) (20), PIV5 strain W3 (PIV5-W3) (22) and PIV5 strain CPI- (PIV5-
114 CPI-) (23). Virus stocks were prepared by inoculating Vero cells at a multiplicity of infection (MOI) of
115 0.001 with continual rocking at 37°C. Supernatants were harvested at 2 d p.i., clarified by
116 centrifugation at 3,000 xg for 15 min, aliquoted and snap-frozen. Titres were estimated by standard
117 plaque assay on Vero cells in 6-well plates.

118 For infection studies, cell monolayers were infected in 6-well plates with virus diluted in medium to
119 achieve a MOI of 10, unless stated otherwise. Virus adsorption was for 1 h, after which the viral
120 inoculum was removed and replaced with media supplemented with 2% (v/v) FBS and incubated in
121 5% (v/v) CO_2 at 37°C until harvested. When cells were treated with IFN-α prior to infection (pre-
122 treated) this was done with 1000 IU/ml IFN-α2b (IntronA, Merck Sharp & Dohme Ltd.) 18 h prior to
123 infection, unless otherwise stated. IFN-α remained on cells for the duration of experiments. Cells
124 were either processed for immunoblot analysis or (if infecting with rPIV5-mCherry, kind gift of Dr He,
125 University of Georgia, USA) imaged using an IncuCyte Zoom imaging system (Sartorius).

126 For plaque assays 30-40 PFU PIV5-CPI- in 1 ml DMEM, 2% FBS were adsorbed for 1 h onto confluent
127 monolayers of cells in 6-well plates while rocking at 37°C. Following adsorption, 2 ml overlay
128 (DMEM, 2% FBS, Avicel) was added to wells and incubated for 6 d. Cells were fixed with 5%
129 formaldehyde (10 min), washed in PBS and permeabilised for 10 min (PBS, 1% Triton X-100, 3% FBS)
130 washed again and incubated for 1 h with a pool of PIV5-specific antibodies (24) diluted in PBS, 3%
131 FBS (1:1000). Following PBS washes, cells were incubated for 1 h with goat anti-mouse IgG
132 antibodies conjugated to alkaline phosphatase (Abcam Cat# ab97020) diluted 1:1000 in PBS, 3%FBS.
133 Cells were washed in PBS and signals were detected using SIGMAFAST BCIP/NBT (Sigma).

134 **Reverse transcription quantitative PCR.**

135 Total cellular RNA was purified from cells that had been treated with 1000 IU/ml IFN-α2b (Intron A)
136 for 18 h, or left untreated, using TRIzol reagent (ThermoFisher Scientific) and Direct-zol RNA

137 Miniprep Plus kits followed by on-column DNase I treatment for the removal of contaminating DNA
138 (Zymo Research). Complementary DNA (cDNA) was synthesised in 20 µl reaction volumes with 500
139 ng total RNA and oligo(dT) using GoScript reverse transcriptase (Promega) according to the
140 manufacturer's recommendations. Quantitative PCR reaction mixes (20 µl) included 1x PerfeCTa
141 SYBR green SuperMix (Quanta BioScience), 0.5 µM each primer and 1 µl cDNA reaction mix. Cycling
142 was performed in a Mx3005P real time PCR machine (Stratagene) and included an initial 3 min
143 enzyme activation step at 95°C, followed by 40 cycles of 10 s at 95°C, 10 s at 58°C and 20 s at 72°C.
144 Melting curve analysis was performed to verify amplicon specificity. Quantification of *β-ACTIN* mRNA
145 was used to normalize between samples and the average cycle threshold (CT) was determined from
146 three independent cDNA samples from independent cultures. Relative expression compared to non-
147 treated control cells was calculated using the ΔΔCT method. Primer sequences were: *HERC5*
148 5'GACGAACTCTTGCACCGTCTC and 5'GCGTCCACAGTCATTTTCCAC, *USP18*
149 5'ATGCTGCCCAACTGTACCTC and 5'CCTGCAGTCTCTCCACCAAG, *MxA* 5'GCCTGCTGACATTGGGTATAA
150 and 5'CCCTGAAATATGGGTGGTTCTC, *IFIT1* 5'CCTGGAGTACTATGAGCGGGC and
151 5'TGGGTGCCTAAGGACCTTGTC, *β-ACTIN* 5'AGCGAGCATCCCCCAAAGTT and
152 5'AGGGCACGAAGGCTCATCATT.

153 **Immunoblotting.**

154 Confluent monolayers in 6-well dishes were lysed with 250 µl 2 x Laemmli sample buffer (4% w/v
155 SDS, 20% v/v glycerol, 0.004% w/v bromophenol blue and 0.125 M Tris-HCl, pH 6.8 with 10% v/v β-
156 mercaptoethanol) for 10 min, incubated at 95°C for 10 min, sonicated at 4°C with 3 cycles of 30 s on
157 30 s off in a Bioruptor Pico (Diagenode) and clarified by centrifugation at 12,000 xg, 4°C for 10 min.
158 SDS-PAGE in Tris-glycine-SDS running buffer and immunoblotting followed standard techniques
159 using the following antibodies: mouse monoclonal anti-ISG15 F-9 (Santa Cruz Biotechnology Cat#
160 sc166755), rabbit polyclonal anti-MxA (Proteintech Cat# 13750-1-AP), goat polyclonal anti-IFIT1 N-16
161 (Santa Cruz Biotechnology Cat# sc82946), mouse monoclonal anti-β-ACTIN, UBA7 (anti-UBE1L B-7;

162 Santa Cruz Biotechnology Cat# sc-390097), mouse monoclonal anti-PIV5 NP 125 (24), mouse
163 monoclonal anti-HPIV2 and anti-PIV5 P 161 (antibody cross-reacts with P of both viruses(24)), mouse
164 monoclonal anti-HPIV3 NP (25). Quantitative immunoblots were analysed using an Odyssey CLx
165 scanner and of membranes incubated with IRDye secondary antibodies (LiCOR). Data were
166 processed using Image Studio software (LiCOR).

167 **^{35}S-methionine labelling.**

168 Subconfluent A549 and A549-ISG15$^{-/-}$ (B8) cells in 6-well plates were treated with 1000 IU/ml IFN-α
169 or left untreated. At 24 h, 48 h and 72 h following treatment cells were pulse-labelled with 500
170 Ci/mmol ^{35}S-Methionine (^{35}S-Met; MP Biomedical) in Met-free media (Sigma) for 1 h. Cells were
171 washed in PBS, lysed in 2 x Laemmli sample buffer and equal amounts of protein were separated by
172 SDS-PAGE. Gels were stained with Coomassie (and imaged to ensure equal loading), dried under
173 vacuum, exposed to a storage phosphor screen and analysed by phoshoimager analysis.

174

175 **Results**

176 **ISG15-knockout A549 cells recapitulate ISG15-deficient patient cells**

177 Among the several immune modulatory roles of ISG15 (8), intracellular ISG15 expression, at least in
178 human cells, is critical for regulating the magnitude of the type I IFN response (10, 14). To investigate
179 the pleotropic nature of human ISG15 we developed cell lines that lack ISG15 expression. Because of
180 our interest in respiratory viruses, including paramyxoviruses, we chose to knockout ISG15
181 expression in the lung adenocarcinoma cell line A549 by CRISPR/Cas9 genome editing as described
182 previously (18). Furthermore, A549 cells have proved to be a very useful model for understanding
183 virus-IFN interactions. The resulting culture was single cell cloned and ISG15 expression was
184 assessed by immunoblotting three clones (B8, B6 and C4). We also selected a clone that had gone
185 through the CRISPR/Cas9 process but retained ISG15 expression (C4+) (Fig. 1a). In addition to control
186 A549 cells, all clones were treated with IFN-α for 24 h, 48 h or left untreated. Immunoblot analysis
187 showed that, compared to control cells, expression of the ISG MxA was higher in A549-ISG15$^{-/-}$ cells
188 (Fig. 1a). We also tested the impact of ISG15-deficiency on the expression of various ISG mRNAs. For
189 this, we selected clone B8 for further analyses; these cells were, in addition to control A549 cells,
190 treated with IFN-α, or left untreated, for 24 h and the expression of various ISGs were examined by
191 RT-qPCR. Whilst IFN-α treatment enhanced the expression of all ISGs tested, this increase was larger
192 in ISG15-deficient cells compared to control A549 cells (between 5- and 10-fold, depending on the
193 ISG) (Fig. 1b). Importantly, the expression of ISGs in non-stimulated cells was equivalent to control
194 cells suggesting that ISG15-dependent regulation is specific to the IFN response and not required for
195 the regulation of basal gene expression. Further experiments showed that lack of ISG15 prolonged
196 the longevity of ISG protein expression, which presumably has an impact on patients with
197 autoinflammatory diseases associated with ISG15 loss-of-function. Here, control A549 and knockout
198 cells were treated with IFN-α for 24 h. The cells were washed and media (without IFN-α) was then
199 added. Cells were harvested every 24 h for 96 h and MxA expression was assessed by

200 immunoblotting (Fig. 1c). In control A549 cells MxA expression peaked at 24 h (the point at which
201 IFN was removed) and had returned to basal levels between 72 and 96 h. In knockout cells MxA
202 expression was clearly higher than in control cells, corroborating our mRNA analyses. Furthermore,
203 while MxA expression in A549-ISG15$^{-/-}$ did recede between 72 and 96 h, high protein levels remained
204 at 96 h. A dysregulated IFN response in ISG15-deficient cells is thought to be due to destabilisation
205 of USP18, a known negative regulator of JAK/STAT signalling (10). To determine if USP18 is similarly
206 affected in our cell lines, A549-ISG15$^{-/-}$ cells were treated with IFN-α for 24 or 48 h (or left untreated)
207 and whole cell lysates were probed for USP18 by immunoblotting. USP18 was robustly induced in
208 A549 cells following IFN-α treatment; however, levels of USP18 were much lower in IFN-α-treated
209 ISG15-deficient cells (Fig. 1d). *USP18* mRNA levels were approximately 10-fold higher in IFN-treated
210 ISG15-deficient cells compared to control A549s, demonstrating that reduced USP18 in A549-ISG15$^{-/-}$
211 cells was not due to reduced transcription (Fig. 1b). Together, these data show that ISG15 is critical
212 for the regulated expression of ISGs. Moreover, they demonstrate that the effects of IFN treatment
213 on our ISG15 knockout A549 cell lines recapitulate the findings in cells derived from ISG15-deficent,
214 patient cells.

215

216 **ISG15-deficiency leads to translational repression following IFN treatment**

217 During our studies we observed that IFN-α-treatment of ISG15-knockout cells led to a reduction in
218 protein synthesis and reasoned that this was a likely contributor to the reported virus resistance in
219 ISG15-deficient cells (14). To investigate this we treated, or left untreated, A549 and A549-ISG15$^{-/-}$
220 (B8) cells with IFN-α. At 24 h, 48 h and 72 h following treatment cells were pulse labelled with ^{35}S-
221 Methionine (^{35}S-Met) for 1 h and the incorporation of ^{35}S-Met was analysed by phoshoimager
222 analysis. These data showed, compared to control cells, that there was a pronounced decrease in
223 protein synthesis in ISG15$^{-/-}$ cells between 24 h and 48 h (Fig. 2a). Furthermore, when cells were pre-
224 treated with IFN-α for 8 h, or left untreated, infected with the orthorubulavirus PIV5 (family

225 *Paramyxoviridae*, sub-family *Orthorubulavirinae*) at a MOI of 10 and then labelled for 1 h with ^{35}S-
226 Met at 24 h and 48 h p.i. (32 h and 56 h post IFN-α treatment, respectively), there was no evidence
227 of viral protein synthesis in treated A549-ISG15$^{-/-}$ cells, whereas in treated control cells, viral protein
228 synthesis was evident at 48 h p.i. (Fig. 2b). These data demonstrate that IFN-treatment of A549-
229 ISG15$^{-/-}$ cells led to inhibition of protein synthesis that was associated with viral resistance, at least at
230 later times.

231

232 **A pre-existing antiviral state in ISG15-deficient cells renders them resistant to parainfluenza virus**
233 **infection**

234 Previous studies have shown that IFN treatment of ISG15-deficient patient cells renders them
235 resistant to viral infection, including the murine respirovirus (family *Paramyxoviridae*, sub-family
236 *Orthoparamyxovirinae*) Sendai virus (14), and this seems to extend to PIV5 with our *in vitro* system
237 (Fig. 2b). To investigate this in A549-ISG15$^{-/-}$ cells, control A549 cells and the ISG15 knockout clones
238 described above were either untreated or treated with 1000 IU/ml IFN-α2b (the same concentration
239 and IFN-α type used in (14)) for 18 h. Cells were then infected with PIV5 (strain W3) (22) for 24 and
240 48 h and analysed by immunoblotting. In all cell lines, the levels of PIV5 nucleoprotein (NP)
241 expression was equivalent at 24 and 48 h in unstimulated cells (Fig. 3a). In IFN-α pre-treated control
242 cells, including C4+ that retained ISG15 expression, the level of NP expression was markedly reduced
243 at 24 h. By 48 h, the level of NP increased showing that infection had progressed even in the
244 presence of IFN-α (Fig. 3a). This is because the PIV5-V protein targets STAT1 for proteasomal
245 degradation, and once sufficient V is expressed, the IFN response is dismantled allowing the virus to
246 replicate (23). However, all A549-ISG15$^{-/-}$ cell lines that had been pre-treated with IFN-α were
247 resistant to PIV5 infection as shown by dramatically reduced, or even absent, NP expression at both
248 time points (Fig. 3a).

249 Previous reports have shown that the ISG15 regulation of IFN signalling is independent of its ability
250 to covalently modify proteins by ISGylation (10). To confirm this, we again applied CRISPR/Cas9
251 genome engineering technology and knocked out expression of UBA7, the E1 enzyme required for
252 ISGylation. For this we took a different approach compared to generating our ISG15 knockout cells
253 (19). Here, we introduced constitutive expression of Cas9 by lentiviral transduction of A549 cells and
254 transduced A549-Cas9 cells with lentiGuide-Puro lentivirus carrying a guide RNA specific for UBA7,
255 followed by single-cell cloning. We confirmed that all clones were UBA7-deficient by immunoblot
256 analysis, which demonstrated that they retained expression of ISG15 but had lost the ability to
257 ISGylate proteins (Fig. 3b). Additionally, following the scheme used in Fig. 3a, these cells were
258 infected with PIV5-W3. These data showed that, compared to ISG15 knockout cells that were
259 resistant to infection, all IFN-α-pre-treated UBA7-knockout cells were infected as efficiently as
260 control cells (Fig. 3b), confirming reports that ISG15-dependent regulation of type I IFN signalling
261 does not require ISGylation (10).

262

263 **The direct antiviral activity of ISGs is responsible for virus resistance**

264 Virus resistance can be induced following 8 h IFN-α treatment (shorter times were not tested), well
265 before any obvious effect on global protein synthesis (Fig. 2). Therefore, shutdown of translation is
266 unlikely to be the sole contributor to virus resistance at early time points and so we wished to
267 determine whether the direct antiviral activity of ISGs was responsible. Addressing this question is
268 complex since, for most viruses, the specific ISG(s) responsible for blocking replication is not known.
269 However, for PIV5, it has been established that IFIT1 is the principle ISG responsible for most of the
270 IFN-dependent antiviral activity (17, 26). We therefore hypothesised that if virus resistance was
271 caused by the direct antiviral activity of ISGs, knockdown of IFIT1 in ISG15-deficient cells would
272 permit PIV5 replication during an antiviral response. We reduced IFIT1 (according to (17)) in A549
273 and A549-ISG15$^{-/-}$ cells and all four cell lines (A549, A549-ISG15$^{-/-}$ and the respective shIFIT1 cells)

274 were pre-treated, or left untreated, with IFN-α and then infected with PIV5-W3 (MOI 10) for 24 and
275 48 h. Expression of PIV5 NP, analysed by quantitative immunoblotting, was used to measure virus
276 infection (Fig. 4a). IFIT1 levels and expression of ISG15 were likewise tested. Typically, pre-treatment
277 of naïve cells with IFN-α reduces infection, as shown by a reduction in NP levels, compared to non-
278 treated cells (Fig. 2b & 3a); nevertheless, because PIV5 expresses the IFN antagonist V protein, NP
279 levels reach similar levels to untreated cells by 48 h p.i. However, this IFN-dependent reduction in
280 virus infection is diminished when IFIT1 is knocked down, confirming earlier reports of IFIT1's
281 antiviral activity against PIV5 (17, 26). While IFN-α pre-treatment of A549-ISG15$^{-/-}$ cells renders them
282 resistant to infection, when IFIT1 was also knocked down, PIV5 infection was restored (Fig. 4a).
283 Because we performed quantitative immunoblotting of NP and β-Actin, we were able to quantify NP
284 levels, allowing us to analyse these changes statistically (Fig. 4b). These data show that in IFN-α-pre-
285 treated cells, knocking IFIT1 down restored NP to similar levels to those seen in untreated cells,
286 regardless of ISG15 status.

287 Rather than solely relying on viral protein expression as a surrogate for virus infection, we also
288 tested virus replication using a biologically relevant plaque assay (Fig. 4c). Cells were infected with
289 approximately 30-40 PFU of PIV5 stain CPI- (PIV5-CPI-) (27), a strain unable to block IFN signalling
290 due to a mutation in its V protein. Infected cells were fixed 6 d p.i. and stained for viral antigen. As
291 previously demonstrated (17), PIV5-CPI- was unable to efficiently form plaques in IFN-competent
292 A549 cells. However, PIV5-CPI- did replicate when cells were unable to produce IFN, such as in A549-
293 Npro cells that constitutively express bovine viral diarrhea virus (BVDV) Npro that cleaves IRF3 (a
294 transcription factor critical for IFN induction (21)). Furthermore, when IFIT1 was knocked down,
295 PIV5-CPI- was able to replicate (albeit less efficiently), further highlighting the major role of IFIT1 as
296 an anti-PIV5 protein. As expected, and like A549 cells, there was very little virus replication in A549-
297 ISG15$^{-/-}$ cells; however, when IFIT1 was knocked down, cells were able to support virus replication. It
298 must be noted however that virus replication in A549-ISG15$^{-/-}$/shIFIT1 cells did not recover to the
299 same degree as A549-shIFIT1 cells. We propose that the reason for this will be complex and may

300 include the likelihood that additional, yet to be identified, anti-PIV5 ISGs exist which are expressed at
301 higher levels in ISG15-deficient cells. Another possible explanation is the inhibition of protein
302 synthesis, including that of viral proteins, in ISG15-deficent cells; cells were infected for 6 days prior
303 to performing the plaque assays, a time point beyond that required to observe a significant effect on
304 protein synthesis (Fig. 2a). Therefore, the plaques observed in A549-ISG15$^{-/-}$/shIFIT1 cells likely result
305 from virus that replicated prior to the inhibition of global protein synthesis.

306 We also investigated infection of these cell lines with other paramyxoviruses whose sensitivity to
307 IFIT1 has been previously reported. Cells were treated with IFN-α and then infected with HPIV2
308 strain Colindale (MOI 10; family *Paramyxoviridae*, sub-family *Orthorubulavirinae*), which is reported
309 to be moderately sensitive to IFIT1-restriction (26), for 24 and 48 h (untreated cells were not
310 analysed because of high cytopathic effect in the absence of IFN). To investigate infection, we
311 detected expression of HPIV2 phosphoprotein by quantitative immunoblotting (Fig. 5a), which
312 showed that IFN-α-pre-treated A549-ISG15$^{-/-}$ cells were largely resistant to infection, although by 48
313 h p.i. there was some, albeit low level, evidence of viral protein accumulation. Nevertheless,
314 infection of A549-ISG15$^{-/-}$/shIFIT1 did allow significantly more viral protein expression. Quantitative
315 analyses demonstrated that viral protein accumulation in A549-ISG15$^{-/-}$/shIFIT1 cells was significantly
316 higher than in A549-ISG15$^{-/-}$ cells, but this was not as high as in A549 control cells, which agrees with
317 the reported partial sensitivity of HPIV2 to IFIT1 restriction indicating that additional ISGs target
318 HPIV2 (Fig. 5b). We performed a similar analysis with HPIV3 strain Washington (20) (family
319 *Paramyxoviridae*, sub-family *Orthoparamyxovirinae*), a virus reported to have limited sensitivity to
320 IFIT1 (26). Interestingly, pre-treatment of A549 and A549-shIFIT1 cells with IFN-α had less of an
321 effect on virus protein accumulation compared to the effects on PIV5 infection (Fig. 5c).
322 Furthermore, while infection of IFN-α-pre-treated ISG15 knockout cells significantly reduced
323 infection compared to control cells, virus infection in these cells was still more robust compared to
324 PIV5 and HPIV2-infected cells. Nevertheless, knockdown of IFIT1 only slightly increased HPIV3

325 protein expression in both ISG15-competent and ISG15-deficient cells (Fig. 5d), supporting reports of
326 a minor role of IFIT1 during the antiviral response to HPIV3 (26).

327 Our data have so far suggested that early virus resistance is mediated by the direct antiviral activity
328 of the IFN response. However, protein synthesis is reduced at later times post-IFN treatment and
329 this is likely to cause resistance; therefore, we investigated whether PIV5 resistance could be
330 induced independently of the direct antiviral activity of IFIT1. To do this we pre-treated the four cell
331 lines (A549, A549-shIFIT1, A549-ISG15$^{-/-}$ and A549-ISG15$^{-/-}$-shIFIT1) with IFN-α for different periods of
332 time, infected with a recombinant PIV5 that expresses the fluorescent protein mCherry (rPIV5-
333 mCherry) for 48 h (MOI 10) and measured fluorescence as a marker of virus replication (Fig. 6a).
334 Virus replication in A549 cells was equivalent regardless of the time cells had been pre-treated with
335 IFN-α and, as expected, A549-ISG15$^{-/-}$ cells were resistant to infection at any time post IFN-α
336 treatment (Fig. 6b). Any advantage to PIV5 replication as a result of IFIT1 knockdown in A549-shIFIT1
337 cells was lost when cells had been pre-treated for 16 h or more, as longer periods of pre-treatment
338 resulted in replication equivalent to IFN-pre-treated A549 cells. Similarly, PIV5 replication in A549-
339 ISG15$^{-/-}$-shIFIT1 cells was higher than A549 control cells, and equivalent to A549-shIFIT1 cells,
340 following 8 and 16 h pre-treatment; however, when cells were pre-treated for 24 h, replication was
341 lower than in A549 and A549-shIFIT1 cells. Interestingly, as the time of pre-treatment of A549-ISG15^{-}
342 $^{/-}$-shIFIT1 cells extended, virus replication reduced further until cells became resistant (e.g. at 60 h
343 and 72 h pre-treatment, Fig. 6b), which was not observed in A549 or A549-shIFIT1 cells. These data
344 suggest that cell permissiveness progressively reduced with longer times of IFN-α pre-treatment,
345 which correlated with the effects of IFN-α treatment on protein synthesis in ISG15-deficient cells
346 (Fig. 2).

347 A previous report demonstrated that ISG15-dependent stabilisation of USP18 was required to bring
348 about regulation of the type I IFN response and this was sufficient for these cells to once again be
349 infected (14). However, what aspects of the antiviral response was responsible for resistance was

350 not investigated. Taken together, these data strongly suggest that virus resistance in early IFN-
351 treated ISG15-deficient cells was caused by the direct antiviral activity of ISGs and not due to a lack
352 of permissiveness as a result of IFN-dependent inhibition of protein synthesis. Nevertheless, because
353 of the reduced protein synthesis in IFN-α-treated ISG15-deficient cells, cells later become non-
354 permissive to infection, even when key ISGs are eliminated.

355

356

357 **Discussion**

358 Previous work had shown that virus resistance was observed in cells that had been treated with IFN-
359 α and then left to rest for 36 h prior to challenge (14). We had observed that IFN-α treatment of
360 A549-ISG15$^{-/-}$ cells led to dramatic decreases in protein synthesis, particularly between 24 and 48 h;
361 therefore, it was not clear whether the initially reported virus resistance was due to defects in
362 translation (including of viral mRNAs) at the timepoint used in (14) or due to the direct antiviral
363 activity of the IFN response. For most viruses, the specific ISG(s) with antiviral activity for a given
364 virus is not known, making the latter difficult to discern; however, for PIV5, it is well established that
365 IFIT1 is responsible for the majority of the antiviral response (17). To study this we generated A549-
366 ISG15$^{-/-}$ cells and showed these cells recapitulated the effects observed in ISG15-deficient patient
367 cells following treatment with IFN-α which included dysregulated ISG expression and reduced USP18
368 protein levels following IFN-α treatment (Fig. 1). Additionally, by knocking-out UBA7, the first
369 enzyme in the ISGylation cascade, we showed that ISGylation is not required for a regulated
370 response (Fig. 3b), confirming previous reports that 'free' ISG15 is required for regulation (10).

371 Using these cell lines in combination with a PIV5 infection model, we showed that infection of IFN-α-
372 pre-treated ISG15-deficient cells in which IFIT1 had been knocked down restored infection, thus
373 confirming that at early times post infection, resistance was indeed due to the direct antiviral activity
374 of the IFN response. Furthermore, because IFIT1 blocks the translation of viral transcripts, our data
375 suggest that IFN-treated A549-ISG15$^{-/-}$ cells were still susceptible to infection, allowing viral
376 transcription to take place prior to IFIT1 restriction, and that ISG15 was unlikely to significantly
377 regulate processes involved in entry. Nevertheless, if ISG15-deficient cells were treated for longer
378 periods with IFN-α prior to infection they did become resistant, even when IFIT1 was knocked down,
379 suggesting that at later times the inhibition of protein synthesis was the principal cause of
380 resistance. These data suggest that the virus resistance reported by Speer et al. (14) was due to a

381 lack of permissiveness and not a result of the direct antiviral activity of the IFN response, although
382 different cells were used in that study.

383 The data here demonstrate that the mechanism of resistance is likely two-fold, depending on the
384 duration that cells are exposed to IFN-α. It is not currently possible to know which mechanism is
385 dominant in ISG15-deicient patients, but it is likely to be a combination of both. Nevertheless, virus
386 resistance results from a lack of IFN signalling control - as a consequence of ISG15-loss-of-function -
387 which would explain why ISG15-deficient patients were not more susceptible to severe infection.
388 This observation, therefore, cannot be used to support the notion that human ISG15 does not
389 possess direct antiviral activity, as proposed (14, 16). It is likely that many viruses will not be
390 sensitive to ISG15-dependent antiviral activity; however, this is true of many antiviral effectors. For
391 example, and as confirmed in this study, IFIT1 strongly restricts PIV5 infection, yet it has reduced
392 activity against HPIV2 and likely no activity against HPIV3 or human respiratory syncytial virus (26). It
393 is also true that several ISGs are often required to limit infection (6); therefore, if one antiviral
394 effector mechanism is absent (such as ISGylation), there is sufficient redundancy to avoid severe
395 effects of infection (redundancy that can complicate the investigation of specific antiviral
396 mechanisms in *in vitro* studies). Nevertheless, several human viruses have been shown to be
397 sensitive to ISGylation and many have evolved specific mechanisms to counteract antiviral
398 ISGylation, adding further weight to the argument that human ISG15 does have antiviral activity
399 (reviewed in (8)). Indeed, other than the handful of patients that have been found to lack ISG15
400 expression (10, 28), individuals will possess an intact IFN response where the antiviral activity of
401 ISG15 (and other effectors) will function, if the infecting virus is sensitive to it.

402 It was surprising that protein synthesis was so affected in ISG15-deficient cells following IFN
403 treatment. It is well established that inhibition of general protein translation is a key feature of the
404 antiviral response and this is through the actions of proteins such as PKR or PERK (PKR-like ER kinase)
405 (4). However, for PKR to be activated it must recognise dsRNA, which was absent in IFN-α-treated

406 cells. Similarly, PERK is activated upon endoplasmic reticulum stress which might be expected during
407 a viral infection, but not following treatment with IFN alone. Previous reports have shown that
408 carcinoembryonic antigen-related cell adhesion molecule 1 (CEACAM1) has antiviral activity against
409 human cytomegalovirus, influenza virus and metapneumovirus by supressing mTOR-mediated
410 protein synthesis (29, 30). The membrane protein CEACAM1 is induced by innate sensors such as
411 TLR-4 (31) and IFI16 (30) and delivers inhibitory signals via SHP1 (haematopoietic cells) or SHP2
412 (epithelial and endothelial cells) phosphatase activity through CEACAM1 immunoreceptor tyrosine-
413 based inhibitory motifs (ITIMs) (32). CEACAM1 expression is rapidly induced following activation of
414 NF-κB and IRF1, but whether IFN-α alone (as used here) can induce it expression is not clear. The
415 *IRF1* promoter possesses a single GAS element, but no IRES, and so its expression is induced by
416 STAT1 homodimers (33). Type I IFN signalling predominantly leads to the formation of STAT1-STAT2
417 heterodimers that associate with IRF9 (to form the ISGF3 transcription factor) to drive expression of
418 ISGs that possess IRES elements in their promoters; however, STAT1 homodimers are formed after
419 type I IFN treatment, but these are at lower concentrations. It is possible that 'late' inhibition of
420 protein synthesis in ISG15-deficient cells (compared to the swifter antiviral activity of IRES-
421 containing genes such as IFIT1) may relate to the kinetics of CEACAM1 expression as the
422 accumulation of STAT1 homodimers is required to drive the expression of *IRF1*, that itself needs to
423 be translated before it induces *CEACAM1*. Of course, the accumulation of STAT1 homodimers may
424 be higher in ISG15-deficient cells because of a dysregulated type I IFN response. Nevertheless, it is
425 plausible that the overamplified type I IFN response in ISG15-deficient cells led to high levels of
426 CEACAM1 (compared to control cells) resulting in inhibition of protein synthesis. Moreover, ISG15
427 may have yet-to-be characterised functions in regulating the cellular response to stressors that lead
428 to inhibition of protein synthesis.

429 It has been reported that ISG15 has a role in regulating the cell cycle through its interactions with
430 SKP2 and USP18, although experiments in that study were not performed in IFN-treated cells, nor
431 were ISG15 knockout cells tested (15). While rates of protein synthesis differ during different stages

432 of the cell cycle, translation is thought to be lowest during mitosis (34). Perturbation of the ISG15-
433 SKP2-USP18 axis following ablation of USP18 led to a delayed progression from G1 to S phase which
434 is not generally thought to be associated with translational repression (35). Of note, we have not
435 observed any obvious differences in cell growth in non-treated A549-ISG15$^{-/-}$ cells. Further work is
436 required to dissect the mechanism responsible for ISG15's effects on general protein translation
437 during an antiviral response.

438 ISG15 has emerged as a central regulator of immunity. It is a pleotropic protein that is strongly
439 expressed following activation of innate immune sensors and connects innate and adaptive
440 immunity. In this study, we have shown that a lack of ISG15 leads to virus resistance by two
441 kinetically distinct mechanisms; the rapid induction of antiviral ISGs and the unexpected effects on
442 protein synthesis. Our newly developed cell lines and infection model will pave the way for further
443 studies investigating the regulatory mechanisms of ISG15 during the antiviral response.

444

445 **Acknowledgments**

446 This work was supported by grants from the Academy of Medical Sciences (SBF003/1028 to DJH),
447 Wellcome Trust Institutional Strategic Support Fund (to DJH), Wellcome Trust (101788/Z/13/Z to
448 RER) and the UK Medical Research Council (MC_UU_12014/1 to JM and CGGB). We are grateful to
449 ERASMUS+ for supporting DH.

450

451 **Figure Legends**

452 **Fig. 1.** Functional characterisation of A549 ISG15 knockout cell lines. (a) CRSIPR/Cas9 genome editing
453 was used to knockout ISG15 expression in A549 cells followed by single-cell cloning (following
454 previously reported procedures (18)). Four independent clones were treated with 1000 IU ml-1 IFN-
455 α for 24 and 48 h, or left untreated, and protein expression was tested by immunoblot analysis of
456 ISG15, MxA and β-Actin. 'Control' cells were naïve A549 cells. Representative image from two
457 independent experiments. (b) A549 and A5549-ISG15$^{-/-}$ (clone B8) were treated with 1000 IU/ml for
458 24 h. Expression of interferon stimulated genes was tested using RT-qPCR with primers specific for
459 *HERC5, USP18, IFIT1* and *MxA*. Relative expression was determined following SYBR green qPCR using
460 ΔΔCt method. *B-Actin* expression was used to normalise between samples. Error bars represent the
461 standard deviation of the mean from three independent RNA samples. (c) A549 and A5549-ISG15$^{-/-}$
462 (clone B8) were treated with 1000 IU/ml for 24 h. Cells were washed and fresh media (without IFN-
463 α) was replaced. Cells were processed for immunoblot analysis using antibodies specific for MxA and
464 β-Actin at 24 h post IFN-α and every 24 h thereafter for 96 h. Controls were cells without IFN-α.
465 Representative image from two independent experiments. (d) A549 and A5549-ISG15$^{-/-}$ (clone B8)
466 were treated with 1000 IU/ml for 24 h and 48 h (or left untreated). Whole cell lysates were analysed
467 by immunoblotting with antibodies specific for USP18, ISG15 and β-Actin. Image is representative of
468 >3 independent experiments.

469

470 **Fig. 2.** Analysis of cellular and viral protein synthesis in ISG15-deficient cells during an antiviral state.
471 (a) Sub-confluent A549 and A549-ISG15$^{-/-}$ (B8) cells were treated with 1000 IU ml^{-1} IFN-α or left
472 untreated. At 24 h, 48 h and 72 h cells were pulsed for 1 h with L-[^{35}S]-Methionine (^{35}S-Met) in Met-
473 free media to metabolically label nascent proteins. Proteins were resolved by SDS-PAGE and stained
474 with Coomassie to ensure equal loading. Labelled proteins were visualised by phophoimager
475 analysis. (b) A549 and A549-ISG15$^{-/-}$ (B8) cells were treated with 1000 IU ml^{-1} IFN-α for 8 h or left

476 untreated and then infected with PIV5 strain W3 (MOI = 10). At 24 or 48 h post infection cells pulsed
477 and processed as in (a). Both experiments were performed independently at least twice.

478

479 **Fig. 3.** A pre-existing antiviral state in ISG15-deficient cells leads to virus resistance which is
480 independent of ISGylation. (a) Control (naïve A549) and 4 independent clones of A549-ISG15$^{-/-}$ cells
481 generated by CRISPR/Cas9 genome editing were treated with 1000 IU/ml IFN-α for 16 h or left
482 untreated and then infected with PIV5 strain W3 (MOI = 10). Cells were harvested at 24 h and 48 h
483 p.i. and processed for immunoblot analysis using antibodies specific for PIV5 nucleoprotein (NP),
484 ISG15, MxA and β-Actin. This experiment was independently performed twice. (b) UBA7 knockout
485 cells were generated using CRISPR/Cas9 genome editing; Cas9-expressing A549 cells were first
486 generated (following transduction with lentiCas9-Blast) and then transduced with lentiGuide-Puro
487 expressing a single guide RNA that targeted exon 3 of the UBA7 gene. Knockout cells were single-cell
488 cloned and three were selected for further analysis. These cells were treated with IFN-α, infected
489 and processed as in (a) using antibodies specific for PIV5 NP, ISG15, UBA7 and β-Actin. This
490 experiment was independently performed twice.

491

492 **Fig. 4.** Direct antiviral activity of ISGs is responsible for virus resistance due to ISG15-loss-of-function.
493 (a) IFIT1 was constitutively knocked down in A549 or A549-ISG15$^{-/-}$ (B8) cells following a previously
494 described method (17). A549, A549-ISG15$^{-/-}$ (B8) and the corresponding IFIT1 knockdown cells were
495 treated with IFN-α, infected with PIV5 and processed as in Fig. 3a. Following immunoblotting with
496 specific antibodies, PIV5 NP and β-Actin were detected using near-infrared (NIR) dye-conjugated
497 secondary antibodies to facilitate quantification. IFIT1 and ISG15 proteins were detected using
498 chemiluminescence following incubation with horseradish peroxidase (HRP)-conjugated secondary
499 antibodies. (b) Experiments described in (a) were performed independently three times (infections
500 were performed on three separate occasions) and NP and β-Actin levels were quantified using Image

501 Studio software (LiCOR). Signals were relative to those generated from IFN-α-treated A549 cells
502 infected for 48 h p.i. (set to 100%). Error bars represent the standard deviation of the mean from the
503 three experiments. ** indicates P < 0.01 using Student's t test. (c) Indicated cells were infected for 1
504 h with 30 – 40 plaque forming units (PFU) of PIV5 (CPI-), a strain unable to block the IFN response
505 due to mutation in V. Monolayers were fixed 6 d p.i. Plaques were detected using a pool of anti-PIV5
506 antibodies specific for hemagglutinin (HN), nucleoprotein (NP), phosphoprotein (P) and matrix
507 protein (M) (see (24)). Plaque assays were performed on 3 independent occasions.

508

509 **Fig. 5.** Restoration of paramyxovirus infection in IFN-α-pretreated ISG15-/- cells reflects their
510 reported sensitivity to IFIT1. (a-b) Experiments were performed as in (Fig. 4a-b). (a) HPIV2 proteins
511 were detected with antibodies specific for HPIV2 P (clone 161; (24)) and NIR-conjugated secondary
512 antibodies. Asterisks denotes non-specific band, arrow denotes HPIV2 P. Samples not treated with
513 IFN-α were omitted due to the highly lytic nature of HPIV2 which hampered their accurate
514 quantification. (b) Quantification of normalised NP signals and compared to the 48 h p.i. sample that
515 was set to 100%. (c) HPIV3 NP proteins were detected using antibodies specific for HPIV3 NP and
516 NIR-conjugated secondary antibodies. (d) Normalised signals were quantified as in (b) and compared
517 to IFN-α-treated, 48 h p.i. samples (set to 100%). Means and standard deviations were derived from
518 three independent experiments performed on different occasions. Asterisks denote statistical
519 significance (* P < 0.05, ** P < 0.01, *** P < 0.001 using Student's t test).

520

521 **Fig. 6.** Virus resistance is induced in ISG15-deficient cells following longer periods of IFN-α pre-
522 treatment. (a) Experimental workflow. (b) Cells were treated 1000 IU ml^{-1} IFN-α in 6-well plates for
523 the indicated times prior to infection. Pre-treated cells were infected with rPIV5-mCherry (MOI 10)
524 for 48 h and mCherry fluorescence was measured using an IncuCyte ZOOM. Background

525 fluorescence from mock-infected wells was subtracted. Data are representative to two independent

526 experiments.

527 **References**

528 1. McFadden, M.J., N.S. Gokhale, and S.M. Horner, Protect this house: cytosolic sensing of
529 viruses. *Curr Opin Virol*, 2017. **22**: p. 36-43.
530 2. Kawai, T. and S. Akira, The role of pattern-recognition receptors in innate immunity: update
531 on Toll-like receptors. *Nat Immunol*, 2010. **11**(5): p. 373-84.
532 3. Randall, R.E. and S. Goodbourn, Interferons and viruses: an interplay between induction,
533 signalling, antiviral responses and virus countermeasures. *J Gen Virol*, 2008. **89**(Pt 1): p. 1-47.
534 4. Dalet, A., E. Gatti, and P. Pierre, Integration of PKR-dependent translation inhibition with
535 innate immunity is required for a coordinated anti-viral response. *FEBS Lett*, 2015. **589**(14):
536 p. 1539-45.
537 5. Mears, H.V. and T.R. Sweeney, Better together: the role of IFIT protein-protein interactions
538 in the antiviral response. *J Gen Virol*, 2018. **99**(11): p. 1463-1477.
539 6. Schoggins, J.W., S.J. Wilson, M. Panis, M.Y. Murphy, C.T. Jones, P. Bieniasz, and C.M. Rice, A
540 diverse range of gene products are effectors of the type I interferon antiviral response.
541 *Nature*, 2011. **472**(7344): p. 481-5.
542 7. Yu, Z.X. and H.M. Song, Toward a better understanding of type I interferonopathies: a brief
543 summary, update and beyond. *World J Pediatr*, 2019.
544 8. Perng, Y.C. and D.J. Lenschow, ISG15 in antiviral immunity and beyond. *Nat Rev Microbiol*,
545 2018. **16**(7): p. 423-439.
546 9. Malakhov, M.P., O.A. Malakhova, K.I. Kim, K.J. Ritchie, and D.E. Zhang, UBP43 (USP18)
547 specifically removes ISG15 from conjugated proteins. *J Biol Chem*, 2002. **277**(12): p. 9976-81.
548 10. Zhang, X., D. Bogunovic, B. Payelle-Brogard, V. Francois-Newton, S.D. Speer, C. Yuan, S.
549 Volpi, Z. Li, O. Sanal, D. Mansouri, I. Tezcan, G.I. Rice, C. Chen, N. Mansouri, S.A. Mahdaviani,
550 Y. Itan, B. Boisson, S. Okada, L. Zeng, X. Wang, H. Jiang, W. Liu, T. Han, D. Liu, T. Ma, B. Wang,
551 M. Liu, J.Y. Liu, Q.K. Wang, D. Yalnizoglu, L. Radoshevich, G. Uze, P. Gros, F. Rozenberg, S.Y.
552 Zhang, E. Jouanguy, J. Bustamante, A. Garcia-Sastre, L. Abel, P. Lebon, L.D. Notarangelo, Y.J.
553 Crow, S. Boisson-Dupuis, J.L. Casanova, and S. Pellegrini, Human intracellular ISG15 prevents
554 interferon-alpha/beta over-amplification and auto-inflammation. *Nature*, 2015. **517**(7532):
555 p. 89-93.
556 11. Francois-Newton, V., G. Magno de Freitas Almeida, B. Payelle-Brogard, D. Monneron, L.
557 Pichard-Garcia, J. Piehler, S. Pellegrini, and G. Uze, USP18-based negative feedback control is
558 induced by type I and type III interferons and specifically inactivates interferon alpha
559 response. *PLoS One*, 2011. **6**(7): p. e22200.
560 12. Malakhova, O.A., K.I. Kim, J.K. Luo, W. Zou, K.G. Kumar, S.Y. Fuchs, K. Shuai, and D.E. Zhang,
561 UBP43 is a novel regulator of interferon signaling independent of its ISG15 isopeptidase
562 activity. *EMBO J*, 2006. **25**(11): p. 2358-67.
563 13. Sarasin-Filipowicz, M., X. Wang, M. Yan, F.H. Duong, V. Poli, D.J. Hilton, D.E. Zhang, and M.H.
564 Heim, Alpha interferon induces long-lasting refractoriness of JAK-STAT signaling in the
565 mouse liver through induction of USP18/UBP43. *Mol Cell Biol*, 2009. **29**(17): p. 4841-51.
566 14. Speer, S.D., Z. Li, S. Buta, B. Payelle-Brogard, L. Qian, F. Vigant, E. Rubino, T.J. Gardner, T.
567 Wedeking, M. Hermann, J. Duehr, O. Sanal, I. Tezcan, N. Mansouri, P. Tabarsi, D. Mansouri,
568 V. Francois-Newton, C.F. Daussy, M.R. Rodriguez, D.J. Lenschow, A.N. Freiberg, D. Tortorella,
569 J. Piehler, B. Lee, A. Garcia-Sastre, S. Pellegrini, and D. Bogunovic, ISG15 deficiency and
570 increased viral resistance in humans but not mice. *Nat Commun*, 2016. **7**: p. 11496.
571 15. Vuillier, F., Z. Li, P.H. Commere, L.T. Dynesen, and S. Pellegrini, USP18 and ISG15
572 coordinately impact on SKP2 and cell cycle progression. *Sci Rep*, 2019. **9**(1): p. 4066.
573 16. Hermann, M. and D. Bogunovic, ISG15: In Sickness and in Health. *Trends Immunol*, 2017.
574 **38**(2): p. 79-93.

575 17. Andrejeva, J., H. Norsted, M. Habjan, V. Thiel, S. Goodbourn, and R.E. Randall, ISG56/IFIT1 is
576 primarily responsible for interferon-induced changes to patterns of parainfluenza virus type
577 5 transcription and protein synthesis. *J Gen Virol*, 2013. **94**(Pt 1): p. 59-68.
578 18. Domingues, P., C.G. Bamford, C. Boutell, and J. McLauchlan, Inhibition of hepatitis C virus
579 RNA replication by ISG15 does not require its conjugation to protein substrates by the
580 HERC5 E3 ligase. *J Gen Virol*, 2015. **96**(11): p. 3236-42.
581 19. Sanjana, N.E., O. Shalem, and F. Zhang, Improved vectors and genome-wide libraries for
582 CRISPR screening. *Nat Methods*, 2014. **11**(8): p. 783-784.
583 20. Durbin, A.P., J.M. McAuliffe, P.L. Collins, and B.R. Murphy, Mutations in the C, D, and V open
584 reading frames of human parainfluenza virus type 3 attenuate replication in rodents and
585 primates. *Virology*, 1999. **261**(2): p. 319-30.
586 21. Hilton, L., K. Moganeradj, G. Zhang, Y.H. Chen, R.E. Randall, J.W. McCauley, and S.
587 Goodbourn, The NPro product of bovine viral diarrhea virus inhibits DNA binding by
588 interferon regulatory factor 3 and targets it for proteasomal degradation. *J Virol*, 2006.
589 **80**(23): p. 11723-32.
590 22. Choppin, P.W., Multiplication of a Myxovirus (Sv5) with Minimal Cytopathic Effects and
591 without Interference. *Virology*, 1964. **23**: p. 224-33.
592 23. Didcock, L., D.F. Young, S. Goodbourn, and R.E. Randall, The V protein of simian virus 5
593 inhibits interferon signalling by targeting STAT1 for proteasome-mediated degradation. *J*
594 *Virol*, 1999. **73**(12): p. 9928-33.
595 24. Randall, R.E., D.F. Young, K.K. Goswami, and W.C. Russell, Isolation and characterization of
596 monoclonal antibodies to simian virus 5 and their use in revealing antigenic differences
597 between human, canine and simian isolates. *J Gen Virol*, 1987. **68 (Pt 11)**: p. 2769-80.
598 25. Rydbeck, R., C. Orvell, A. Love, and E. Norrby, Characterization of four parainfluenza virus
599 type 3 proteins by use of monoclonal antibodies. *J Gen Virol*, 1986. **67 (Pt 8)**: p. 1531-42.
600 26. Young, D.F., J. Andrejeva, X. Li, F. Inesta-Vaquera, C. Dong, V.H. Cowling, S. Goodbourn, and
601 R.E. Randall, Human IFIT1 Inhibits mRNA Translation of Rubulaviruses but Not Other
602 Members of the Paramyxoviridae Family. *J Virol*, 2016. **90**(20): p. 9446-56.
603 27. Chen, C., R.W. Compans, and P.W. Choppin, Parainfluenza virus surface projections:
604 glycoproteins with haemagglutinin and neuraminidase activities. *J Gen Virol*, 1971. **11**(1): p.
605 53-8.
606 28. Bogunovic, D., M. Byun, L.A. Durfee, A. Abhyankar, O. Sanal, D. Mansouri, S. Salem, I.
607 Radovanovic, A.V. Grant, P. Adimi, N. Mansouri, S. Okada, V.L. Bryant, X.F. Kong, A. Kreins,
608 M.M. Velez, B. Boisson, S. Khalilzadeh, U. Ozcelik, I.A. Darazam, J.W. Schoggins, C.M. Rice, S.
609 Al-Muhsen, M. Behr, G. Vogt, A. Puel, J. Bustamante, P. Gros, J.M. Huibregtse, L. Abel, S.
610 Boisson-Dupuis, and J.L. Casanova, Mycobacterial disease and impaired IFN-gamma
611 immunity in humans with inherited ISG15 deficiency. *Science*, 2012. **337**(6102): p. 1684-8.
612 29. Diab, M., A. Vitenshtein, Y. Drori, R. Yamin, O. Danziger, R. Zamostiano, M. Mandelboim, E.
613 Bacharach, and O. Mandelboim, Suppression of human metapneumovirus (HMPV) infection
614 by the innate sensing gene CEACAM1. *Oncotarget*, 2016. **7**(41): p. 66468-66479.
615 30. Vitenshtein, A., Y. Weisblum, S. Hauka, A. Halenius, E. Oiknine-Djian, P. Tsukerman, Y.
616 Bauman, Y. Bar-On, N. Stern-Ginossar, J. Enk, R. Ortenberg, J. Tai, G. Markel, R.S. Blumberg,
617 H. Hengel, S. Jonjic, D.G. Wolf, H. Adler, R. Kammerer, and O. Mandelboim, CEACAM1-
618 Mediated Inhibition of Virus Production. *Cell Rep*, 2016. **15**(11): p. 2331-9.
619 31. Muenzner, P., M. Naumann, T.F. Meyer, and S.D. Gray-Owen, Pathogenic Neisseria trigger
620 expression of their carcinoembryonic antigen-related cellular adhesion molecule 1
621 (CEACAM1; previously CD66a) receptor on primary endothelial cells by activating the
622 immediate early response transcription factor, nuclear factor-kappaB. *J Biol Chem*, 2001.
623 **276**(26): p. 24331-40.
624 32. Gray-Owen, S.D. and R.S. Blumberg, CEACAM1: contact-dependent control of immunity. *Nat*
625 *Rev Immunol*, 2006. **6**(6): p. 433-46.

626 33. Michalska, A., K. Blaszczyk, J. Wesoly, and H.A.R. Bluyssen, A Positive Feedback Amplifier
627 Circuit That Regulates Interferon (IFN)-Stimulated Gene Expression and Controls Type I and
628 Type II IFN Responses. *Front Immunol*, 2018. **9**: p. 1135.
629 34. Polymenis, M. and R. Aramayo, Translate to divide: small es, Cyrillicontrol of the cell cycle by
630 protein synthesis. *Microb Cell*, 2015. **2**(4): p. 94-104.
631 35. Stumpf, C.R., M.V. Moreno, A.B. Olshen, B.S. Taylor, and D. Ruggero, The translational
632 landscape of the mammalian cell cycle. *Mol Cell*, 2013. **52**(4): p. 574-82.

633

634

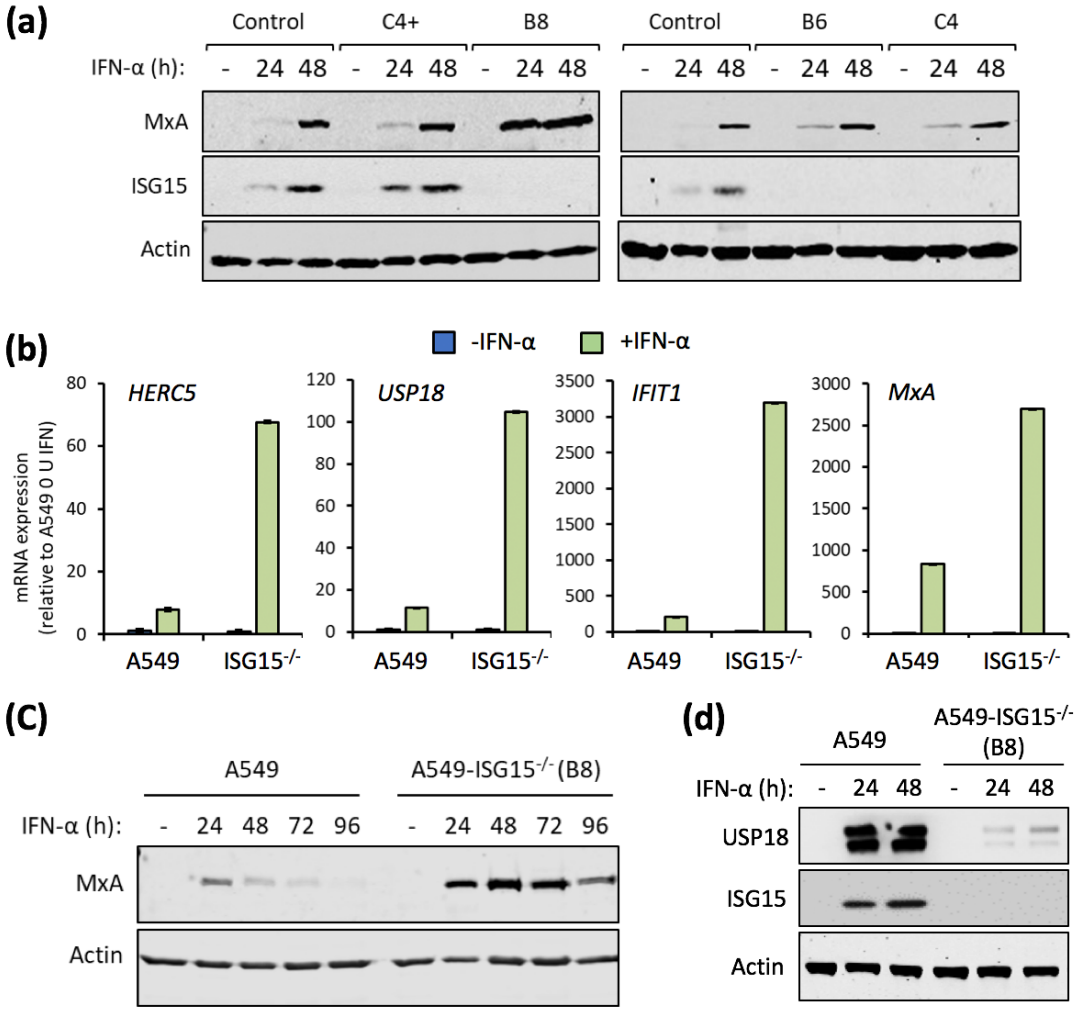

Figure 1. Functional characterisation of A549 ISG15 knockout cell lines. (a) CRSIPR/Cas9 genome editing was used to knockout ISG15 expression in A549 cells followed by single-cell cloning (following previously reported procedures (18)). Four independent clones were treated with 1000 IU ml-1 IFN-α for 24 and 48 h, or left untreated, and protein expression was tested by immunoblot analysis of ISG15, MxA and β-Actin. 'Control' cells were naïve A549 cells. Representative image from two independent experiments. (b) A549 and A5549-ISG15$^{-/-}$ (clone B8) were treated with 1000 IU/ml for 24 h. Expression of interferon stimulated genes was tested using RT-qPCR with primers specific for *HERC5, USP18, IFIT1* and *MxA*. Relative expression was determined following SYBR green qPCR using ΔΔCt method. *B-Actin* expression was used to normalise between samples. Error bars represent the standard deviation of the mean from three independent RNA samples. (c) A549 and

646 A5549-ISG15$^{-/-}$ (clone B8) were treated with 1000 IU ml^{-1} for 24 h. Cells were washed and fresh
647 media (without IFN-α) was replaced. Cells were processed for immunoblot analysis using antibodies
648 specific for MxA and β-Actin at 24 h post IFN-α and every 24 h thereafter for 96 h. Controls were
649 cells without IFN-α. Representative image from two independent experiments. (d) A549 and A5549-
650 ISG15$^{-/-}$ (clone B8) were treated with 1000 IU ml^{-1} for 24 h and 48 h (or left untreated). Whole cell
651 lysates were analysed by immunoblotting with antibodies specific for USP18, ISG15 and β-Actin.
652 Image is representative of >3 independent experiments.

653

654

655

656

657

658

659

660

661

662

663

664

665

666

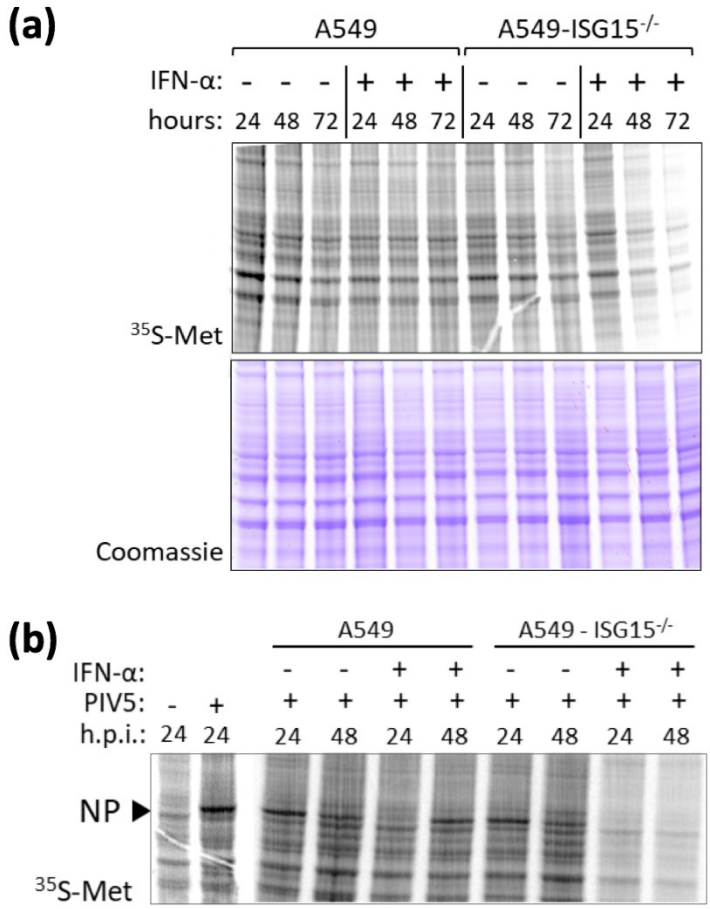

Figure 2. Analysis of cellular and viral protein synthesis in ISG15-deficient cells during an antiviral state. (a) Sub-confluent A549 and A549-ISG15$^{-/-}$ (B8) cells were treated with 1000 IU ml-1 IFN-α or left untreated. At 24 h, 48 h and 72 h cells were pulsed for 1 h with L-[^{35}S]-Methionine (^{35}S-Met) in Met-free media to metabolically label nascent proteins. Proteins were resolved by SDS-PAGE and stained with Coomassie to ensure equal loading. Labelled proteins were visualised by phophoimager analysis. (b) A549 and A549-ISG15$^{-/-}$ (B8) cells were treated with 1000 IU/ml IFN-α for 8 h or left untreated and then infected with PIV5 strain W3 (MOI = 10). At 24 or 48 h post infection cells pulsed and processed as in (a). Both experiments were performed independently at least twice.

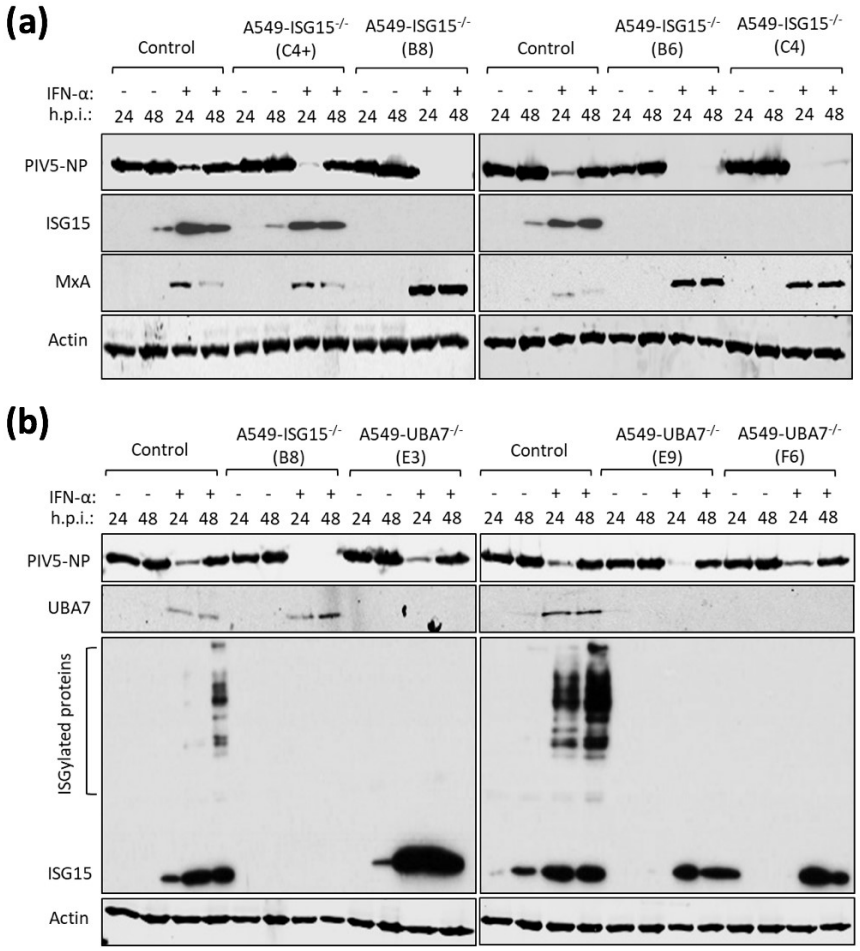

Figure 3. A pre-existing antiviral state in ISG15-deficient cells leads to virus resistance which is independent of ISGylation. (a) Control (naïve A549) and 4 independent clones of A549-ISG15$^{-/-}$ cells generated by CRISPR/Cas9 genome editing were treated with 1000 IU/ml IFN-α for 16 h or left untreated and then infected with PIV5 strain W3 (MOI = 10). Cells were harvested at 24 h and 48 h p.i. and processed for immunoblot analysis using antibodies specific for PIV5 nucleoprotein (NP), ISG15, MxA and β-Actin. This experiment was independently performed twice. (b) UBA7 knockout cells were generated using CRISPR/Cas9 genome editing; Cas9-expressing A549 cells were first generated (following transduction with lentiCas9-Blast) and then transduced with lentiGuide-Puro expressing a single guide RNA that targeted exon 3 of the UBA7 gene. Knockout cells were single-cell cloned and three were selected for further analysis. These cells were treated with IFN-α, infected and processed as in (a) using antibodies specific for PIV5 NP, ISG15, UBA7 and β-Actin. This experiment was independently performed twice.

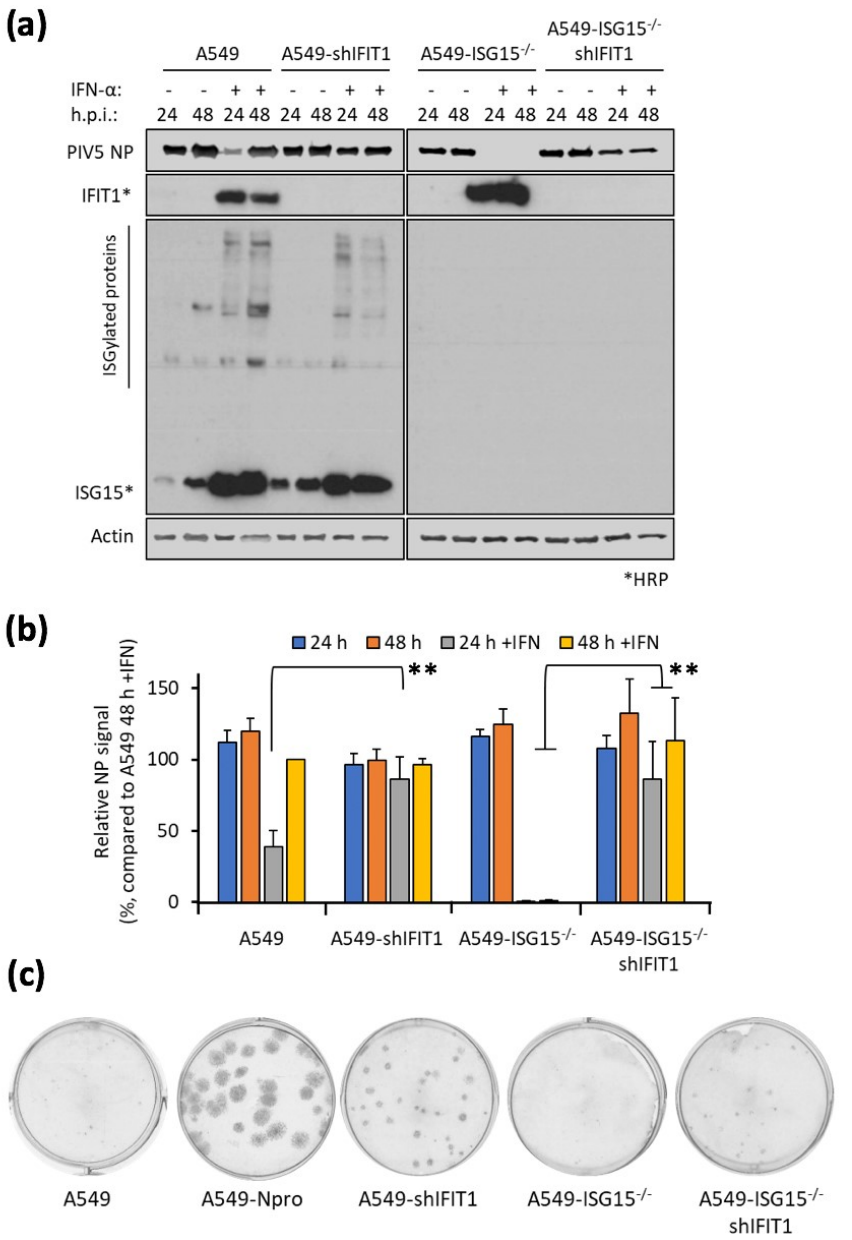

692

693 **Figure 4.** Direct antiviral activity of ISGs is responsible for virus resistance due to ISG15-loss-of-
694 function. (a) IFIT1 was constitutively knocked down in A549 or A549-ISG15$^{-/-}$ (B8) cells following a
695 previously described method [17]. A549, A549-ISG15$^{-/-}$ (B8) and the corresponding IFIT1 knockdown
696 cells were treated with IFN-α, infected with PIV5 and processed as in Fig. 3a. Following
697 immunoblotting with specific antibodies, PIV5 NP and β-Actin were detected using near-infrared
698 (NIR) dye-conjugated secondary antibodies to facilitate quantification. IFIT1 and ISG15 proteins were
699 detected using chemiluminescence following incubation with horseradish peroxidase (HRP)-
700 conjugated secondary antibodies. (b) Experiments described in (a) were performed independently

701 three times (infections were performed on three separate occasions) and NP and β-Actin levels were
702 quantified using Image Studio software (LiCOR). Signals were relative to those generated from IFN-α-
703 treated A549 cells infected for 48 h p.i. (set to 100%). Error bars represent the standard deviation of
704 the mean from the three experiments. ** indicates $P < 0.01$ using Student's t test. (c) Indicated cells
705 were infected for 1 h with 30 – 40 plaque forming units (PFU) of PIV5 (CPI-), a strain unable to block
706 the IFN response due to mutation in V. Monolayers were fixed 6 d p.i. Plaques were detected using a
707 pool of anti-PIV5 antibodies specific for hemagglutinin (HN), nucleoprotein (NP), phosphoprotein (P)
708 and matrix protein (M) (see [24]). Plaque assays were performed on 3 independent occasions.

709

710

711

712

713

714

715

716

717

718

719

720

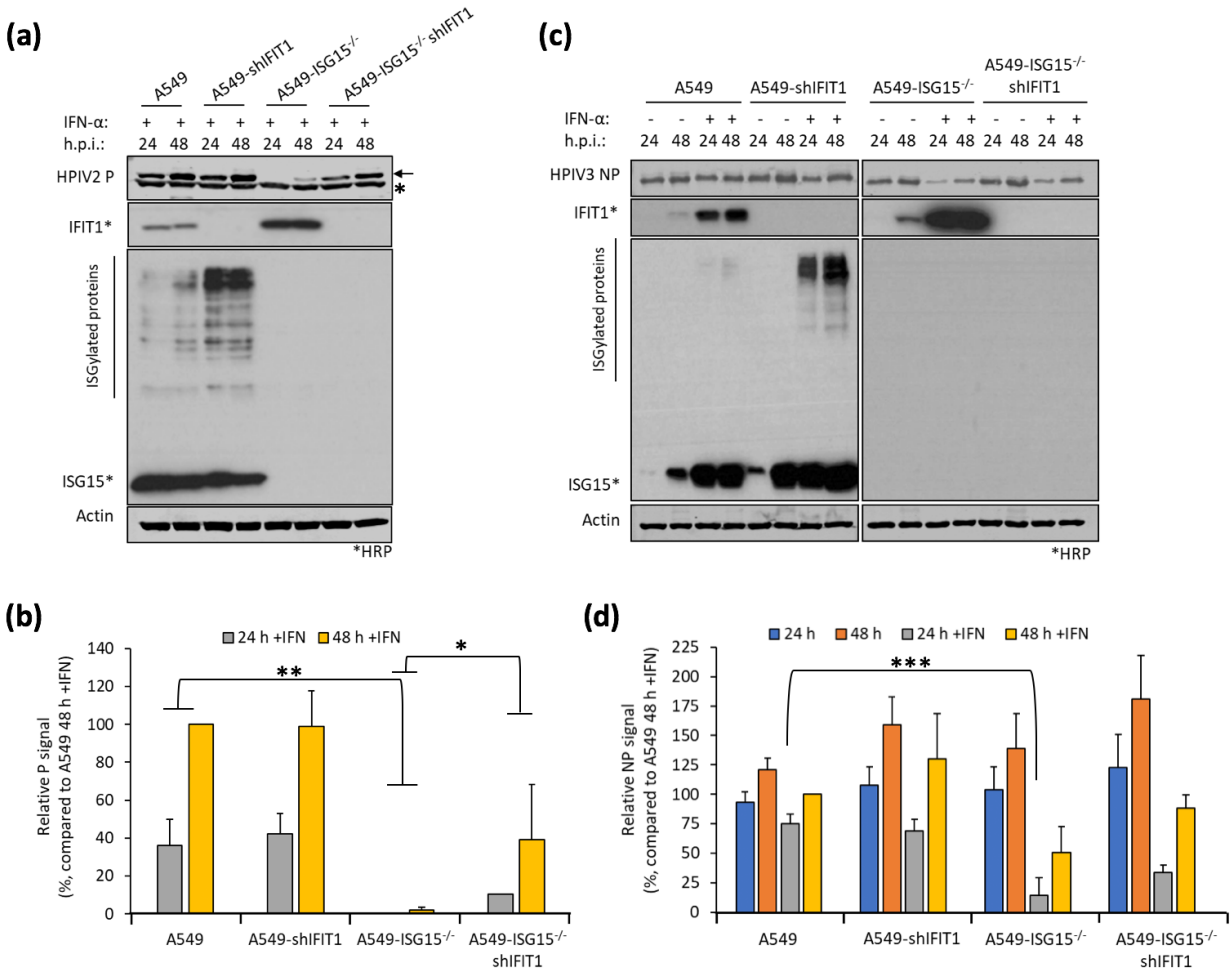

Figure 5. Restoration of paramyxovirus infection in IFN-α-pretreated ISG15$^{-/-}$ cells reflects their reported sensitivity to IFIT1. (a-b) Experiments were performed as in (Fig. 4a-b). (a) HPIV2 proteins were detected with antibodies specific for HPIV2 P (clone 161; [24]) and NIR-conjugated secondary antibodies. Asterisks denotes non-specific band, arrow denotes HPIV2 P. Samples not treated with IFN-α were omitted due to the highly lytic nature of HPIV2 which hampered their accurate quantification. (b) Quantification of normalised NP signals and compared to the 48 h p.i. sample that was set to 100%. (c) HPIV3 NP proteins were detected using antibodies specific for HPIV3 NP and NIR-conjugated secondary antibodies. (d) Normalised signals were quantified as in (b) and compared to IFN-α-treated, 48 h p.i. samples (set to 100%). Means and standard deviations were derived from three independent experiments performed on different occasions. Asterisks denote statistical significance (* $P < 0.05$, ** $P < 0.01$, *** $P < 0.001$ using Student's t test).

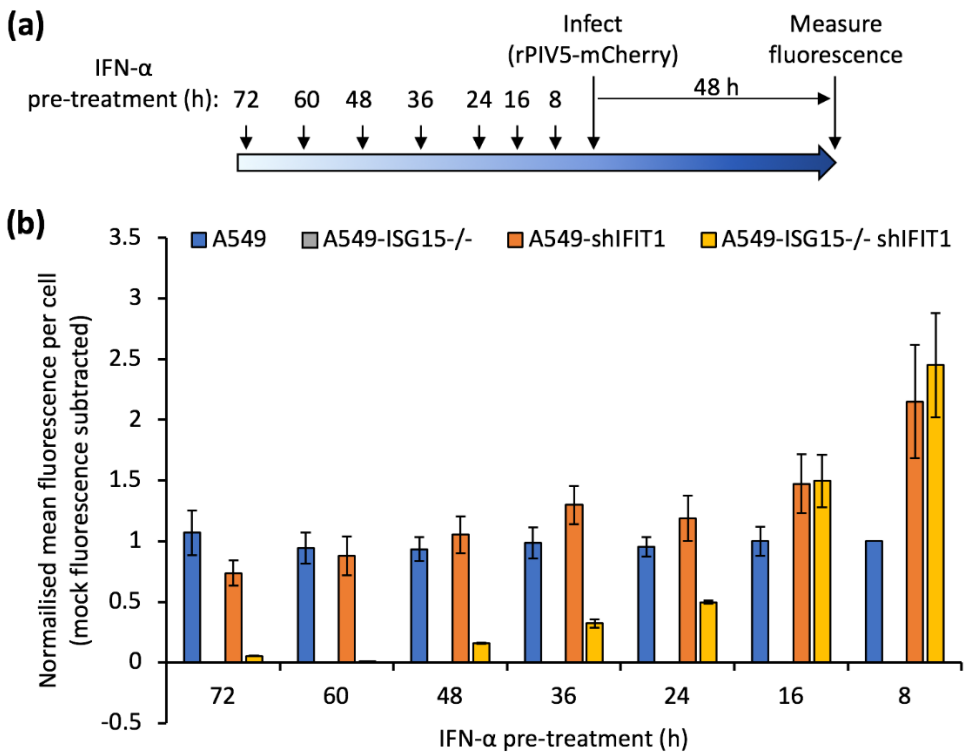

733

734 **Figure 6.** Virus resistance is induced in ISG15-deficient cells following longer periods of IFN-α pre-

735 treatment. (a) Experimental workflow. (b) Cells were treated 1000 IU ml-1 IFN-α in 6-well plates for

736 the indicated times prior to infection. Pre-treated cells were infected with rPIV5-mCherry (MOI 10)

737 for 48 h and mCherry fluorescence was measured using an IncuCyte ZOOM. Background

738 fluorescence from mock-infected wells was subtracted. Data are representative to two independent

739 experiments.